Key Engineering Materials
ISSN: 1662-9795, Vol. 926, pp 2238-2246
doi:10.4028/p-1n7iop

Submitted: 2021-12-13
Revised: 2022-01-26
Accepted: 2022-01-28
Online: 2022-07-22

Parameter Identification of Swift Law Using a FEMU-Based Approach and an Innovative Heterogeneous Mechanical Test

M. Conde[1,a*], J. Henriques[1,b], S. Coppieters[2,c], A. Andrade-Campos[1,d]

[1]Centre of Mechanical Technology and Automation (TEMA), Department of Mechanical Engineering, University of Aveiro, Portugal

[2]Department of Materials Engineering, Ghent Technology Campus, KU Leuven, Belgium

[a]marianaconde@ua.pt, [b]joaodiogofh@ua.pt, [c]sam.coppieters@kuleuven.be, [d]gilac@ua.pt

Keywords: Parameter identification; Heterogeneous specimen; FEMU; DIC; FEM.

Abstract. The reliability and predictive accuracy of forming simulation depend on both the material constitutive model and its inherent parameters. As opposed to conventional sheet metal material testing, heterogeneous mechanical tests provide more complex strain and stress states. Heterogeneous mechanical tests can be used to efficiently predict the material behavior in forming processes due to an improvement in the time required and accuracy in the identification of the parameters. The present work aims at identifying the Swift hardening law parameters of a dual-phase steel by means of an optimum-designed interior notched specimen that presents several strain and stress states simultaneously. The finite element model updating (FEMU) technique was used for the identification of 3 parameters, by comparing a DIC-measured virtual material with numerical results iteratively DIC-filtered.

Introduction, Framework and Literature Review

The simulation and virtualization of manufacturing processes are crucial for the development of engineering solutions. However, realistic simulation predictions require an adequate constitutive model and the accurate determination of its inherent parameters. Nowadays, its calibration relies on several classical mechanical tests. This approach is very time and cost consuming. Besides, it only provides information for a fixed stress state that cannot reassemble the complex strain and stress fields that are generated in many manufacturing processes [1]. On contrary, the heterogeneous mechanical tests can provide several strain and stress states simultaneously, reducing the required number of tests in the model calibration [2]. Several authors ([1-10]) have already proved the reliability of the heterogeneous mechanical tests for model calibration using inverse methods. Moreover, it was proved in [5, 7 and 11] that these tests outperform the classical tests in parameter identification.

Regarding parameter identification, various methods can be used and, for further information, it is recommended to read the review in [12]. An adaptation of the Finite Element Model Updating (FEMU) is going to be used in this work. The FEMU is an optimization procedure that compares the strain/displacement fields or even the reaction force of the experimental test with a numerical test by calculating its difference. Nevertheless, it is not consistent to compare experimental data that was measured using Digital Image Correlation (DIC) with numerical data obtained with FEA since there are several discrepancies, such as different coordinate systems, data locations, strain formulation and calculation methods, spatial resolution and filtering [13]. Significant strain errors were observed in [13] when comparing results using direct interpolation methods due to disregarding the effect of the DIC filtering. These issues can lead to errors in the FEMU cost function value, which are reported in [14]. So, in this work, the FEMU approach was adapted to measure the strain fields of the numerical test with DIC techniques. This way, both experimental and numerical sets of data have the same filtering, spatial resolution and strain calculation method. Besides, in this work, the experimental test was replaced by a virtual test obtained using synthetically deformed images based on the data of a numerical test, as in [15]. Thus, the error between the obtained set of parameters and the reference can be estimated.

It is very important to have adequate input data for the FEMU. Therefore, an innovative heterogeneous mechanical test for uniaxial loading conditions developed in [16] using an optimization approach based on a heterogeneity indicator is going to be used for the parameter identification of the Swift law. Although it seems unnecessary to use a heterogeneous test for the calibration of the Swift law, it was concluded otherwise with the methodology present in [17]. The influence of the parameters on the strain gradients was evaluated and it was demonstrated that a more heterogeneous test presents better identifiability of these parameters when compared to a test with reduced heterogeneity. Moreover, this approach allows the identification of the material parameters beyond the onset of necking, which is the classical experimental limit.

This paper is divided into four sections. The first presents a short introduction, framework on the topic and a literature review. The second section describes the methodology and implementation. There's a description of the heterogeneous mechanical tests and the heterogeneous dogbone test (for comparison reasons) used for the parameter identification, the constitutive model that was calibrated and the material used. Subsequently, the Finite Element Analysis (FEA) model of the tests, the DIC and synthetic images technique and lastly the adapted FEMU-based approach are presented. The third section presents the analysis and results of the parameter identification of the Swift hardening law with both tests. The last section offers the conclusions and the proposal of future works.

Methodology and Implementation

A FEMU-based approach was used to identify the parameters of Swift hardening law regarding DP600 steel. However, some adaptations of the classical FEMU technique were made for this work. Generally, this approach compares experimental with numerical data. Though, the experimental data was replaced by virtual experimental data which information was calculated using DIC and synthetically deformed images, being considered the material of reference. This way, it is possible to estimate the error between the calibrated solution and the reference solution. Additionally, the iteratively numerically generated data is not compared directly with the reference material data. Again, synthetically deformed images were created iteratively based on the numerical analysis, being the numerical data a DIC-leveled numerical data. Therefore, both solutions are evaluated using the same measurement technique. A flowchart showing all the process here described is presented in Figure 1.

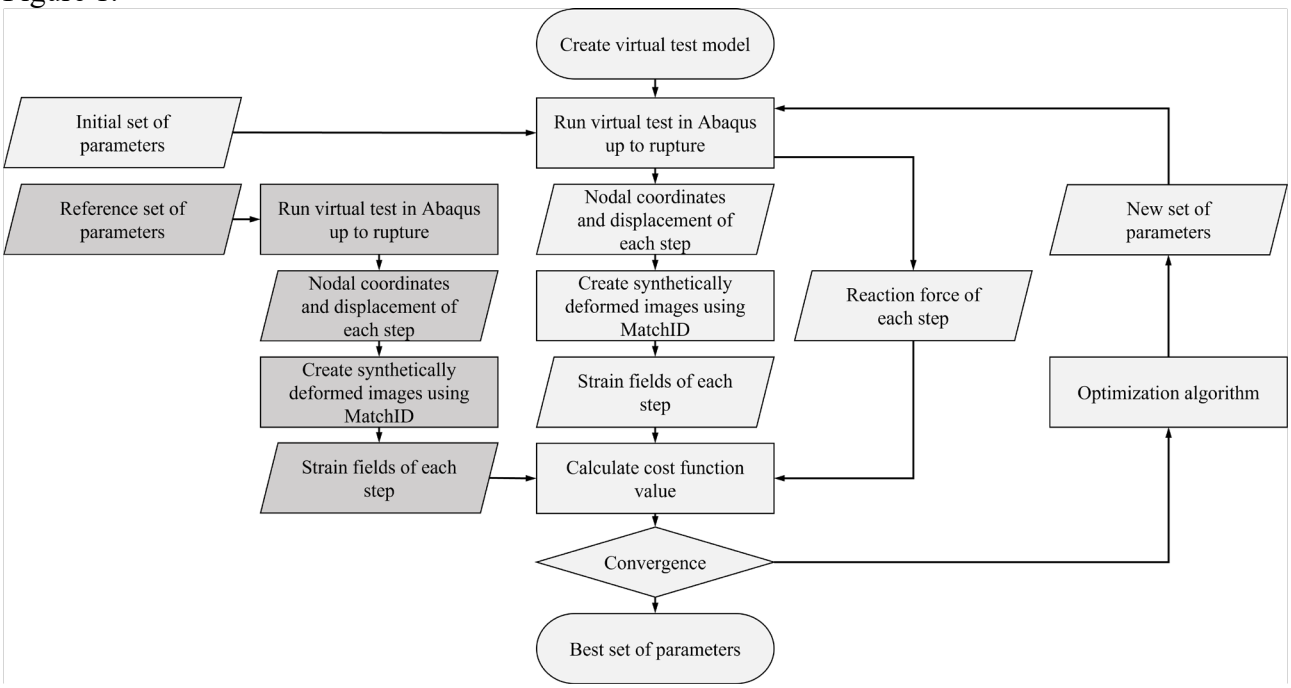

Figure 1: Flowchart describing the FEMU-based approach using a full integration of the synthetically deformed images to identify the unknown set of parameters of the material constitutive model.

Mechanical Tests. In the present work, synthetically deformed images of an innovative heterogeneous mechanical test proposed in [16 and 18] were used as reference virtual material data in the approach. Moreover, for comparison reasons, a heterogeneous dogbone test was also analyzed. Its non-constant section geometry and uniaxial loading conditions are presented in Figure 2 (a).

The geometry of the heterogeneous specimen is presented in Figure 2 (b). This interior notched specimen was design by shape optimization, based on the maximization of the heterogeneity. The heterogeneity of the test was evaluated using several heterogeneity indicators that favor solutions that exhibit several strain states simultaneously with large magnitudes. The shape of the interior notch follows a third-degree spline defined by a total of 20 points, which coordinated of the first quadrant are presented in Table 1. This specimen has 2 symmetries, ensuring the balance during the experimental testing. The specimen is tested in uniaxial loading conditions up to rupture.

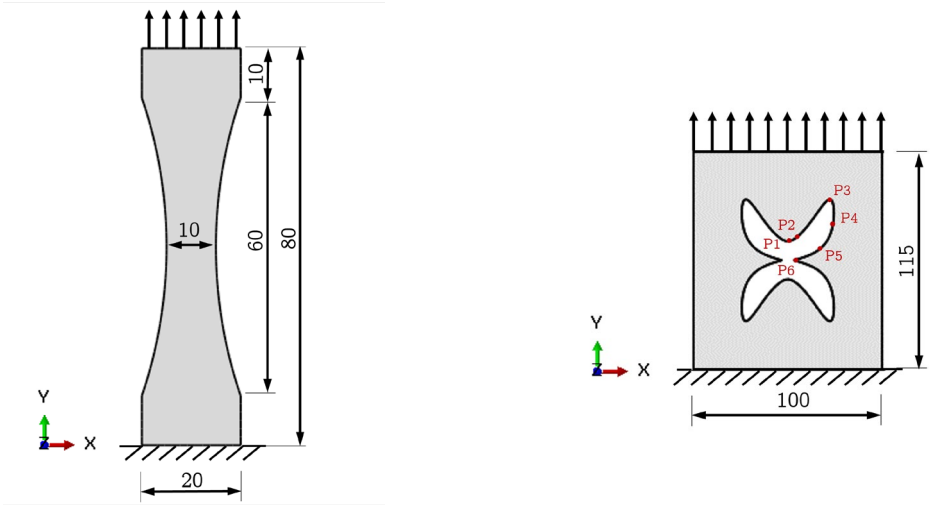

(a) (b)

Figure 2: Geometry, dimensions (in mm) and loading conditions of the specimen (a) for the dogbone mechanical test and (b) for the heterogeneous mechanical test used in the parameter identification approach.

Table 1: Geometry definition of the interior notch shape in the first quadrant. Coordinates of the spline considering the origin located in the center of the specimen.

	P1	P2	P3	P4	P5	P6
xx [mm]	0.000	3.708	23.092	23.505	15.889	3.086
yy [mm]	10.000	11.412	31.784	17.078	5.163	0.000

Constitutive Model and Material Definition. To describe the numerical linear elastic material behavior, the Hooke's law was used, with a modulus of elasticity of 210 GPa and Poisson's ratio of 0.3. For the hardening and anisotropy behavior, it was defined the Swift hardening law [19] and the Yld2000-2d criterion [20], respectively. The reference parameters of the DP600 steel with 0.8 mm thickness are presented in Table 2. The rupture criterion implemented was based on the FLD (Forming Limit Diagram) [21]. Only the parameters of the Swift law were calibrated, being a total of 3 parameters. The exponential of the Yld2000-2d function nominated as a is equal to 6 since the material has a BCC type of crystal structure.

Table 2: Swift hardening law and Yld200-2d criterion parameters of the reference solution [21].

Swift Law	K [MPa]			ε_0			n		
	979.460			0.00535			0.194		
Yld 2000-2d	α_1	α_2	α_3	α_4	α_5	α_6	α_7	α_8	a
	1.011	0.964	1.191	0.995	1.01	1.018	0.977	0.935	6

Finite Element Analysis of the Test. The mechanical tests previously specified were modeled using Abaqus software [22] under plane stress state using 858 and 2975 CPS4R elements for the dogbone and for the heterogeneous specimen, respectively. The type of numerical element used was the CPS4R. The material behavior was implemented using the UMMDp developed by JANCAE (Japan Association of Nonlinear CAE) [23]. Both specimens were subjected to uniaxial loading conditions by imposing a displacement up to rupture. A total of 10 evenly spaced time increments were used to create the synthetic images.

DIC and Synthetic Images. The MatchID 2D software [24] was used to synthetically deform a speckle pattern, based on the initial mesh and displacement fields outputted from the Abaqus simulation. The speckle pattern was numerically generated with a 3 px dot size to avoid aliasing [25] and printed in true dimensions. The hardware and DIC analysis parameters are presented in Table 3. A performance analysis was conducted to access the adequate DIC parameters, which are presented in the same table.

Table 3: Hardware and DIC analysis parameters using MatchID 2D software [24].

Parameters	
Camera	Flir Blackfly BFS-U3-51S5M-C
Image resolution [px^2]	2448×2048
Focal length [mm]	12.5
Average speckle size [px]	3
Image filtering	Gaussian, 5px kernel
Image conversion factor [mm/px]	0.05039 (for the dogbone test); 0.07241 (for the heterogeneous test)
Subset size [px]	21
Step size [px]	5
Subset shape function	Quadratic
Matching criterion	ZNSSD
Interpolation	Bi-cubic spline
Strain window [datapoints]	11
Strain formulation	Green-Lagrange
Post-filtering of strains	Spatial
Displacement noise-floor [px]	0.009
Strain noise-floor [mm/mm]	1.246×10^{-4} (for the dogbone test); 1.209×10^{-4} (for the heterogeneous test)

FEMU-Based Approach.

The FEMU-based approach is driven by the minimization of the optimization function written as:

$$\varphi(\boldsymbol{\chi}) = \frac{1}{n_\mathrm{t}} \sum_{i=1}^{n_\mathrm{t}} \left\{ \frac{1}{3n_\mathrm{p}} \sum_{j=1}^{n_\mathrm{p}} \left[\left(\frac{\varepsilon_{xx}^{\mathrm{num}}(\boldsymbol{\chi}) - \varepsilon_{xx}^{\mathrm{exp}}}{\varepsilon_{\max}^{\mathrm{exp}}} \right)^2 + \left(\frac{\varepsilon_{yy}^{\mathrm{num}}(\boldsymbol{\chi}) - \varepsilon_{yy}^{\mathrm{exp}}}{\varepsilon_{\max}^{\mathrm{exp}}} \right)^2 + \left(\frac{\varepsilon_{xy}^{\mathrm{num}}(\boldsymbol{\chi}) - \varepsilon_{xy}^{\mathrm{exp}}}{\varepsilon_{\max}^{\mathrm{exp}}} \right)^2 \right]_j + \right.$$
$$\left. + \left(\frac{F^{\mathrm{num}}(\boldsymbol{\chi}) - F^{\mathrm{exp}}}{F_{\max}^{\mathrm{exp}}} \right)^2 \right\}_i, \tag{1}$$

where $\boldsymbol{\chi}$ is the vector of the unknown set of material parameters, F is the load signal and ε is the originated strains obtained after a DIC analysis. The superscripts "num" and "exp" refer to the data originated iteratively during the optimization process and the virtual experimental (reference) data, respectively. The number of time instances is n_t and the number of in-plane measurement points is n_p. $F_{\max}^{\mathrm{ref}}$ is the maximum load value for each test and $\varepsilon_{\max}^{\mathrm{ref}}$ the maximum strain value of all in-plane components for each test.

The optimization algorithm used was the Levenberg-Marquardt [26], which is a robust optimization algorithm that is generally used to solve non-linear least squares problems.

Analysis and Results

The DIC-levelled FEMU approach was analyzed for different initial sets of parameters and the optimized solutions were obtained. The maximum and minimum bounds in between which each parameter can vary are presented in Table 4, as well as the best parameters and the relative errors of the model calibrated with the dogbone and the heterogeneous specimens.

Table 4: Reference set of parameters, minimum and maximum admissible bounds, initial and final set of parameters and relative error compared to the reference of the adapted FEMU calibration using the dogbone and heterogeneous specimens.

	K [MPa]	ε_0	n	Cost function
Minimum bound	500.00	0.100×10^{-5}	0.100×10^{-5}	-
Maximum bound	1500.0	0.0100	0.400	-
Heterogeneous dogbone test				
Reference set	979.46	0.00535	0.194	1.055×10^{-9}
Initial set 1	1000.0	0.00480	0.100	7.099×10^{-2}
Final set	942.96	9.99×10^{-7}	0.169	2.689×10^{-4}
Error [%]	3.7265	100	12.9	-
Initial set 2	708.51	0.00573	0.218	8.830×10^{-2}
Final set	979.14	0.00534	0.194	1.680×10^{-8}
Error [%]	0.032671	0.187	0.000	-
Heterogeneous test				
Reference set	979.46	0.00535	0.194	2.665×10^{-8}
Initial set 1	1000.0	0.00480	0.100	8.853×10^{-2}
Final set	902.99	0.00457	0.103	5.153×10^{-2}
Error [%]	7.8069	14.6	46.9	-
Initial set 2	708.51	0.00573	0.218	8.612×10^{-2}
Final set	979.00	0.00533	0.194	3.323×10^{-8}
Error [%]	0.046964	0.374	0.000	-

Although there is a notable dependence of the initial set of parameters in the identification process, a significant reduction of the cost function value was obtained with both test configurations. The dogbone test identifies the parameters with a relative error below 0.2%, whereas the heterogeneous test finds the parameters with relative errors below 0.4%. Both calibrations are very accurate, especially in the identification of the n parameter. Also, in both approaches, the identified parameter with the largest relative errors is the ε_0. The large errors obtained with the initial set 1 can be reduced by changing the initial set of parameters and attempting a multi-starting approach.

The evolution of each material parameter, the cost function and the strain and force terms of the cost function along the identification process for the set of calibrated parameters that displays the lowest relative error (started from the initial set 2) is shown in Figure 3. It can be noticed that the 3 parameters are accurately identified after 50 evaluations. The cost function value is lower for the dogbone approach mainly due to the larger reduction of the differences in the strain fields. This can be associated with the complexity of the generated gradients. Indeed, the dogbone specimen yields a strain field that can be easily reconstructed by the DIC algorithm. The heterogeneous specimen, however, generates strong strain gradients which are much more challenging for strain reconstruction. Concerning the force term, it presents similar behavior between both tests. Regarding the computational time, the heterogeneous test takes approximately 2.5 times more computational time than the dogbone test for each evaluation.

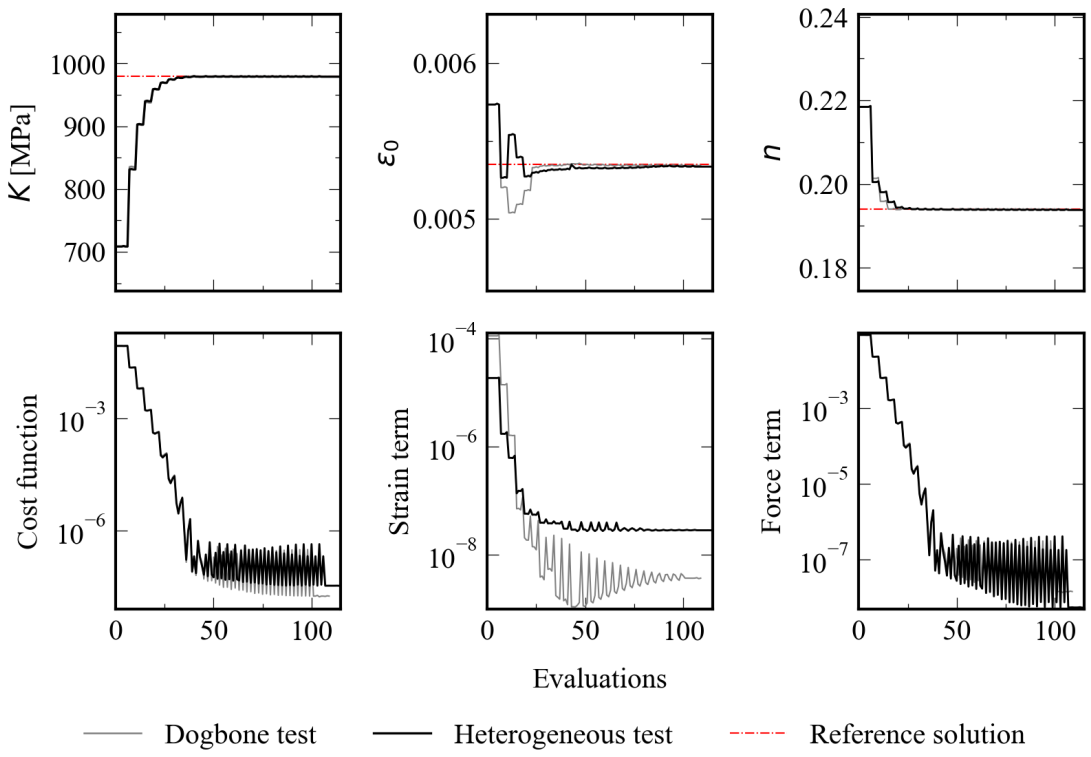

Figure 3: Evolution of the material parameters, cost function and strain and force term of the cost function value along the identification process of the initial set 2.

The same set of parameters was used to plot the Swift hardening law, depicted in Figure 4. Again, it is observed that both calibrations are very accurate, comparing to the reference solution.

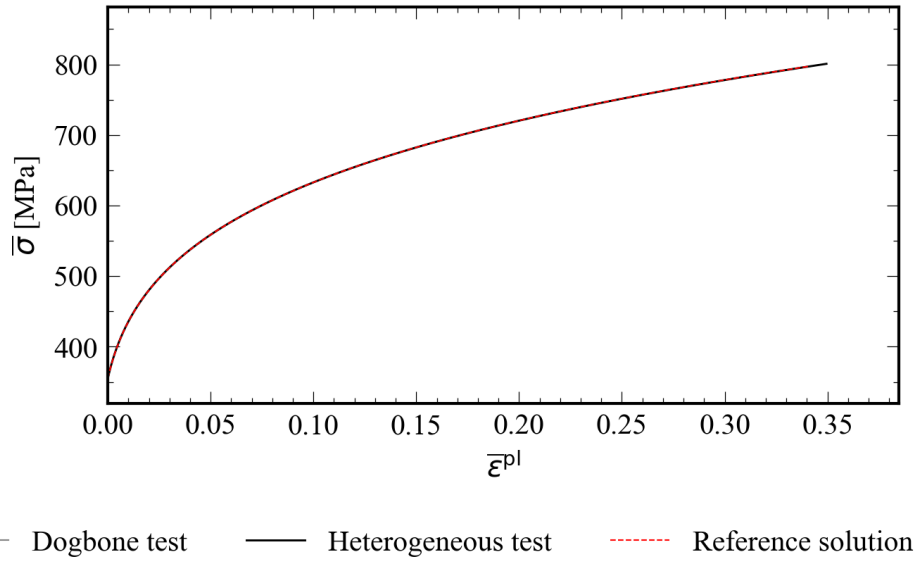

Figure 4: Swift hardening law representation of the calibrated parameters of the initial set 2.

In this case, the heterogeneous test is as accurate as the dogbone test to calibrate the Swift law. However, it is expected for the heterogeneous test to better calibrate an anisotropy constitutive model, since it presents several different strain and stress states, that the dogbone does not.

Conclusions and Future Works

In the present work, the Swift hardening law parameters were identified using an innovative heterogeneous specimen and a heterogeneous dogbone specimen, both under uniaxial loading conditions up to rupture. A total of 3 parameters were accurately calibrated using a DIC-levelled

FEMU methodology. Both the experimental (virtual experiment, for this work) and the numerical strain fields are evaluated through DIC-filtered deformed synthetic images, using Abaqus and MatchID 2D software's, respectively.

In terms of the identification problem, both the dogbone test and the heterogeneous test approaches found the best set of parameters after 50 evaluations. The optimization process is very dependent on the initial set of parameters and, thus it is not robust. Even so, this problem was overcome using more than one initial set of parameters. There were found very accurate material parameters of the Swift hardening law, with relative errors below 0.4% for both the dogbone and heterogeneous test. These sets of parameters correctly represent the Swift law curve, compared to the reference set of parameters. The main differences observed in the cost function value were related to the strain term. This is probably due to the simpler strain gradients that the dogbone test exhibits and can be better reconstructed. While the heterogeneous test presents a more complex strain field, that can lead to larger errors in the strain field virtual reconstruction.

The different strain and stress states that the heterogeneous test can display were not relevant to calibrate the hardening model, but it is expected to become essential in reducing the number of experimental tests necessary for the accurate calibration of a more complex constitutive model, for instance when identifying anisotropy behavior of materials.

As future works, it is proposed to extend this methodology to the identification of a more complex constitutive model, such as the Yld2000-2d function. In this case, it is expected to be necessary to evaluate different material orientations and several dogbone tests in order to have a correct model calibration. Concerning the heterogeneous test, it is expected to reduce the number of required tests, compared to the heterogeneous dogbone test, since the first presents more complex strain and stress fields.

Acknowledgments

This project has received funding from the Research Fund for Coal and Steel under grant agreement No 888153.

The authors also gratefully acknowledge the financial support of the Portuguese Foundation for Science and Technology (FCT) under the projects CENTRO-01-0145-FEDER-029713, POCI-01-0145-FEDER-031243 and POCI-01-0145-FEDER-030592 by UE/FEDER through the programs CENTRO 2020 and COMPETE 2020, and UIDB/00481/2020 and UIDP/00481/2020-FCT under CENTRO-01-0145-FEDER-022083. Mariana Conde is grateful to the Portuguese Foundation for Science and Technology (FCT) for the PhD grant 2021.06115.BD.

References

[1] S. Cooreman, D. Lecompte, H. Sol, J. Vantomme, and D. Debruyne, "Identification of mechanical material behavior through inverse modeling and DIC," *Exp. Mech.*, vol. 48, no. 4, pp. 421–433, 2008, doi: 10.1007/s11340-007-9094-0.

[2] S. Cooreman, "Identification of the plastic material behaviour through full-field displacement measurements and inverse methods," Free University of Brussels, Belgium, 2008.

[3] J. Kajberg and G. Lindkvist, "Characterisation of materials subjected to large strains by inverse modelling based on in-plane displacement fields," *Int. J. Solids Struct.*, vol. 41, no. 13, pp. 3439–3459, 2004, doi: 10.1016/j.ijsolstr.2004.02.021.

[4] T. Pottier, F. Toussaint, and P. Vacher, "Contribution of heterogeneous strain field measurements and boundary conditions modelling in inverse identification of material parameters," *Eur. J. Mech. A/Solids*, vol. 30, no. 3, pp. 373–382, 2011, doi: 10.1016/j.euromechsol.2010.10.001.

[5] T. Pottier, P. Vacher, F. Toussaint, H. Louche, and T. Coudert, "Out-of-plane Testing Procedure for Inverse Identification Purpose: Application in Sheet Metal Plasticity," *Exp. Mech.*, vol. 52, no. 7, pp. 951–963, 2012, doi: 10.1007/s11340-011-9555-3.

[6] J. H. Kim, F. Barlat, F. Pierron, and M. G. Lee, "Determination of Anisotropic Plastic Constitutive Parameters Using the Virtual Fields Method," *Exp. Mech.*, vol. 54, no. 7, pp. 1189–1204, 2014, doi: 10.1007/s11340-014-9879-x.

[7] P. A. Prates, M. C. Oliveira, and J. V. Fernandes, "A new strategy for the simultaneous identification of constitutive laws parameters of metal sheets using a single test," *Comput. Mater. Sci.*, vol. 85, pp. 102–120, 2014, doi: 10.1016/j.commatsci.2013.12.043.

[8] N. M. Souto, "Computational design of a mechanical test for material characterization by inverse analysis," University of Aveiro, Portugal, 2015.

[9] S. Zhang, L. Léotoing, D. Guines, and S. Thuillier, "Potential of the Cross Biaxial Test for Anisotropy Characterization Based on Heterogeneous Strain Field," *Exp. Mech.*, vol. 55, no. 5, pp. 817–835, 2015, doi: 10.1007/s11340-014-9983-y.

[10] E. M. C. Jones *et al.*, "Parameter covariance and non-uniqueness in material model calibration using the Virtual Fields Method," *Comput. Mater. Sci.*, vol. 152, pp. 268–290, 2018, doi: 10.1016/j.commatsci.2018.05.037.

[11] S. Cooreman, "Identification of the plastic material behaviour through full-field displacement measurements and inverse methods," no. September, p. 191, 2008.

[12] S. Avril *et al.*, "Overview of identification methods of mechanical parameters based on full-field measurements," *Exp. Mech.*, vol. 48, no. 4, pp. 381–402, 2008, doi: 10.1007/s11340-008-9148-y.

[13] P. Lava, E. M. C. Jones, L. Wittevrongel, and F. Pierron, "Validation of finite-element models using full-field experimental data : Levelling finite-element analysis data through a digital image correlation engine," *Strain*, vol. 56, no. e12350, 2020, doi: 10.1111/str.12350.

[14] J. Henriques, João;Conde, Mariana; Andrade-Campos, António; Xavier, "Identification of Swift law parameters using FEMU by a synthetic image approach based on digital image correlation," in *Esaform 2022 - 25th International Conference on Material Forming*, 2022.

[15] M. Rossi, P. Lava, F. Pierron, D. Debruyne, and M. Sasso, "Effect of DIC spatial resolution, noise and interpolation error on identification results with the VFM," *Strain*, vol. 51, no. 3, pp. 206–222, 2015, doi: 10.1111/str.12134.

[16] M. Conde, A. Andrade-Campos, M. G. Oliveira, and J. M. P. Martins, "Design of heterogeneous interior notched specimens for material mechanical characterization," in *Esaform 2021 - 24th International Conference on Material Forming*, 2021, doi: 10.25518/esaform21.2502.

[17] Y. Zhang, S. Gothivarekar, M. Conde, A. Van de Velde, A. Andrade-Campos, and S. Coppieters, "Enhancing the information-richness of specimens for identification of plastic anisotropy through full-field strain fields," *Int. J. Mech. Sci.*, vol. 214, no. 7, p. 106891, 2021, doi: 10.1016/j.ijmecsci.2021.106891.

[18] M. Conde, "Design of a heterogeneous interior notched specimen using shape optimisation approach," University of Aveiro, Portugal, 2020.

[19] H. W. Swift, "Plastic instability under plane stress," *J. Mech. Phys. Solids*, vol. 1, no. 1, pp. 1–18, 1952.

[20] F. Barlat *et al.*, "Plane stress yield function for aluminum alloy sheets - Part 1: Theory," *Int. J. Plast.*, vol. 19, no. 9, pp. 1297–1319, 2003, doi: 10.1016/S0749-6419(02)00019-0.

[21] F. Ozturk, S. Toros, and S. Kilic, “Effects of anisotropic yield functions on prediction of forming limit diagrams of DP600 advanced high strength steel,” *Procedia Eng.*, vol. 81, no. October, pp. 760–765, 2014, doi: 10.1016/j.proeng.2014.10.073.

[22] Dassault Systèmes, “Abaqus 6.14 Online Documentation,” 2014. [Online]. Available: http://ivt-abaqusdoc.ivt.ntnu.no:2080/texis/search/?query=wetting&submit.x=0&submit.y=0&group=bk&CDB=v6.14. [Accessed: 25-Mar-2020].

[23] H. Takizawa, T. Kuwabara, K. Oide, and J. Yoshida, “Development of the subroutine library ‘UMMDp’ for anisotropic yield functions commonly applicable to commercial FEM codes,” *J. Phys. Conf. Ser.*, vol. 734, no. 3, 2016, doi: 10.1088/1742-6596/734/3/032028.

[24] MatchID, “New MatchID release 2021.1,” 2021. [Online]. Available: https://www.matchid.eu/Software.html. [Accessed: 25-Jun-2021].

[25] International Digital Image Correlation Society, E. M. C. Jones, and M. . Iadicola, *A Good Practices Guide for Digital Image Correlation*. 2018.

[26] S. Community, “Optimization - scipy.optimize,” *SciPy.org*, 2021. [Online]. Available: https://docs.scipy.org/doc/scipy/reference/tutorial/optimize.html. [Accessed: 01-Oct-2021].